.

FGF/MAPK signaling pathway regulates the genome-wide occupancy of Polycomb Repressive Complex 2 in murine embryonic stem cells

Short title: FGF/MAPK signaling regulates PRC2 occupancy

Mohammad B. Aljazi[1], Yuen Gao[1], Yan Wu[1], George I. Mias[1,2], Jin He[1*]

[1]Department of Biochemistry & Molecular Biology, College of Nature Sciences, Michigan State University, East Lansing, MI 48824

[2]Institute for Quantitative Health Science and Engineering, Michigan State University, East Lansing, MI 48824

*To whom correspondence should be addressed

Phone: 517-353-0613

Email: hejin1@msu.edu

Abstract

Previous studies demonstrated that genome-wide PRC2 occupancy is largely reduced in primitive mESCs cultured in 2 inhibitors-containing medium. To understand the underlying mechanisms, we performed RNA-sequencing analyses to show the expression of Jarid2 and Eed is significantly reduced in primitive mESCs due to blocking of the FGF/MAPK pathway. ChIP-seq analyses showed that decreased genome-wide occupancy of Ezh2 and H3K27me3 modification is correlated with a global reduction of Jarid2 occupancy. The ectopic expression of Jarid2 partially restores both global PRC2 occupancy and H3K27me3 modification. Further gene expression analyses showed the reduced global PRC2 occupancy does not lead to de-repression of lineage differentiation genes in primitive mESCs. Together, these results revealed the FGF/MAPK signaling pathway is critical in determining the global PRC2 occupancy through regulating the expression of PRC2 components. The reduced Jarid2-mediated PRC2 recruitment is the main molecular mechanism leading to the global reduction of PRC2 occupancy in primitive mESCs.

Introduction

Polycomb repressive complexes (PRCs) are critical for maintaining mouse embryonic stem cells (mESCs) in an undifferentiated state by repressing lineage-specific gene expression(*1-3*). Previous studies have shown that both PRC1 and PRC2 are recruited to the silenced gene promoters and mediate monoubiquitylation of histone H2A lysine 119 (H2AK119ub1) and trimethylation of histone H3 lysine 27 (H3K27me3) respectively(*4-6*). The promoters bound by PRCs have a high transcriptional threshold, which prevents stochastic transcriptional activation of lineage-specific genes in mESCs(*7*).

Although the genome-wide occupancy of PRCs in mESCs has been well documented, the molecular mechanisms for recruiting PRCs to specific genomic loci in mammalian cells have not fully elucidated. A variety of factors, such as Jarid2 and Mtf2, have been reported to mediate the PRC2 recruitment(*8-13*). On the other hand, Kdm2b is able to recruit a PRC1.1 variant to the mammalian unmethylated CpG islands (CGIs) through its CxxC-ZF domain(*14-16*). Recently, Kdm2b was also reported to recruit PRC2 though the interaction of Jarid2/PRC2 with Kdm2b/PRC1.1-mediated histone H2AK119ub1 modification(*17*).

mESCs cultured in serum-containing medium are capable of maintaining their self-renewal and undifferentiation status(*18*). However, differentiation-inducing signals such as the MAPK signaling triggered by fibroblast growth factors (FGFs) in the serum induce low-level expression of early lineage-specific genes. After being cultured in 2i serum-free medium in which the FGF/MAPK signaling is chemically inhibited, mESCs turn to a primitive state with a reduced basal expression of early lineage-specific genes(*19, 20*). Along with the gene expression changes, primitive mESCs display two major genome-wide epigenetic changes(*21*): (i) a global reduction of DNA methylation mainly due to decreased expression of Uhrf1 and loss of DNA methylation maintenance(*22, 23*), and (ii) both genome-wide PRC2 occupancy and its mediated histone H3K27me3 modification are drastically reduced(*24, 25*). Although the exact mechanisms for the reduced PRC2 occupancy in primitive mESCs are unknown, one postulated hypothesis is the new DNA demethylated regions in primitive mESCs are bound by Kdm2b, which further re-localizes PRC2 to the ectopic sites. Consequently, the PRC2 occupancy at the canonical CGIs is decreased(*26*).

To examine the proposed hypothesis, we performed RNA-sequencing (RNA-seq) analyses to compare the gene expression in wild-type mESCs cultured in serum versus 2i medium. The results showed that the expression of a core PRC2 component Eed and a known PRC2 recruiting factor Jarid2 is significantly reduced in primitive mESCs, which is further confirmed by both quantitative reverse transcription and polymerase chain reaction (qRT-PCR) and western blot (WB) analyses. Reactivation of FGF/MAPK signaling increases the expression of Jarid2 and Eed, suggesting the FGF/MAPK signaling positively regulates their expression. Chromatin immunoprecipitation coupled with deep sequencing (ChIP-seq) analyses showed that the global occupancy of Ezh2 and histone H3K27me3 modification are largely reduced in primitive mESCs, which is correlated with a global reduction of Jarid2 occupancy. In contrast, the genome-wide Kdm2b occupancy does not have marked changes. The ectopic expression of Jarid2 in primitive mESCs could partially restore the global Ezh2 occupancy and increase the H3K27me3 modification. At the transcriptional level, the RNA-seq analyses showed that the PRC2-regulated early lineage-specific genes are not derepressed in primitive mESCs even through the PRC2 occupancy at gene promoters is reduced. Together, this study revealed that the FGF/MAPK signaling plays a critical role in determining the global PRC2 occupancy by regulating the expression of core PRC2 components in mESCs. The reduced global PRC2 occupancy in primitive mESCs is likely to be caused by the reduced Jarid2-mediated PRC2 recruitment but not the Kdm2b-mediated PRC2 re-localization to ectopic DNA demethylated regions.

Results

1. The expression of Jarid2 and Eed is significantly reduced in primitive mESCs

The reduced global PRC2 occupancy in primitive mESCs could be caused by the reduced expression of PRC2 components. To investigate this possibility, we performed RNA-seq analyses to examine the differential gene expression between wild-type mESCs cultured in serum containing medium (ESC-S) and 2i medium (ESC-2i). The results identified a total of 2255 upregulated genes and 2476 downregulated genes in ESC-2i respectively (cutoff: 1.5 fold expression change and $p < 0.01$) (Fig. 1A, 1B). Consistent with previous reports, Nanog, Klf4, and Prdm14 are found to be upregulated in the ESC-2i, validating the proper 2i culture condition and the primitive status of mESCs in the study (Fig. 1C)(*27-29*). Notably, both Jarid2 and Eed are found to have significant reduced expression in mESC-2i compared to that in mESC-S (Fig. 1D). Other PRC1 and PRC2 components including Kdm2b, Ring1b, Ezh1, Ezh2, Suz12, and Mtf2 do not show statistically significant differences in expression between mESC-S and mESC-2i (Fig.S1A, B). The reduced expression of Jarid2 and Eed is further confirmed by both qRT-PCR

and WB analyses at the mRNA and protein levels (Fig. 1E-1H). Based on these results, we concluded that the expression of PRC2 components Jarid2 and Eed is significantly reduced in primitive mESCs.

2. FGF/MAPK signaling positively regulates the expression of Jarid2 and Eed

The FGF/MAPK signaling is blocked by the removal of serum and supplement of MEK inhibitor PD0325901 in 2i medium. To examine whether the reduced expression of Jarid2 and Eed is caused by the deficiency of FGF/MAPK signaling in 2i medium, we added the fetal bovine serum back to, and removed the MEK inhibitor PD0325901 from the 2i medium. RNA-seq analyses were performed to examine the gene expression at different time points after the medium change (Fig. 2A). The activation of FGF/MAPK signaling is monitored by WB analyses on the phosphorylated MAPK p42/44. The result showed that the phosphorylated MAPK p42/44 are not detected in the ESC-2i. However, the phosphorylated proteins quickly increase and reach to a constant level at 6 hours after the medium switch, confirming the reactivation of FGF/MAPK signaling (Fig. 2B). The RNA-seq analyses at 0, 6 and 12 hours after the medium change identified total 309 genes upregulated in response to the activation of FGF/MAPK signaling (Fig. 2C). Kyoto Encyclopedia of Genes and Genomes (KEGG) pathway analysis revealed that the upregulated genes are enriched in the MAPK signaling pathway, signaling involved in regulating stem cell pluripotency, signaling pathway in cancer, and HIF signaling pathway, further confirming that the FGF/MAPK signaling pathway is properly activated in mESCs after the medium change (Fig. 2D, Table S1). Notably, RNA-seq results showed that both Jarid2 and Eed increase their expression in response to the reactivation of FGF/MAPK signaling pathway (Fig.2E, S2A,2B). The increased expression of Jarid2 and Eed is further confirmed by qRT-PCR and WB analyses at the mRNA and protein levels (Fig. 2F-2H). Based on these results, we concluded that the FGF/MAPK signaling positively regulates the expression of Jarid2 and Eed and blocking of this signaling pathway in the 2i medium leads to their reduced expression at both mRNA and protein levels in primitive mESCs.

3. The genome-wide PRC2 occupancy is largely reduced in primitive mESCs

To examine the Polycomb occupancy and the histone modifications in primitive mESCs, we performed ChIP-seq analyses to compare the global occupancy of Jarid2, Ezh2, Kdm2b, Ring1b and histone H3K27me3/H3K4me3 modifications in mESC-S and mESC-2i. Since Polycomb complexes and Mll1/Mll2 complexes are recruited to CGIs in mammalian cells, we measured the overall Polycomb occupancy and histone H3K27me3/H3K4me3 modifications by calculating the

total normalized mapped reads within 10kb-window flanking entire CGI regions. Consistent with previous reports(*24, 25*), both genome-wide PRC2 occupancy and histone H3K27me3 modification are largely reduced in primitive mESCs, which is correlated well with the global decreased Jarid2 occupancy (Fig. 3A-3C, 3E). In contrast, the global H3K4me3 modification is slightly increased in the mESC-2i (Fig. S3A). Also, in contrast to the Ezh2 occupancy that is reduced at both GGIs and their flanking sites, the occupancy of PRC1 core component Ring1b is mainly reduced at the CGI flanking regions but not the CGI center (Fig.3B). Of note, the ChIP-seq results demonstrated that Kdm2b has similar genome-wide occupancy at CGIs in mESC-S and mESC-2i (Fig. 3D, 3E). Since Kdm2b has similar expression levels in mESCs cultured in these two conditions (Fig. S1A, 1B), this result indicates that Kdm2b is less likely to have genome-wide re-localization from canonical CGIs to new ectopic DNA demethylated regions in primitive mESCs. Together, these results suggest that reduced Jarid2 and Eed expression is likely to be the main factor leading to the reduced global PRC2 occupancy and histone H3 modification in primitive mESCs.

4. Ectopic expression of Jarid2 partially restores the global PRC2 occupancy and histone H3K27me3 modification in primitive mESCs

To further confirm that the reduced Jarid2 expression is the main causing factor leading to the global reduction of PRC2 occupancy in primitive mESCs, we rescued the Jarid2 expression in primitive mESCs by lentiviral viruses expressing puromycin resistant cassette fused with Jarid2 by a self-cleaved P2A sequence. After transduction, the transduced cells were selected by adding puromycin in the medium. RNA-seq analyses showed that the Jarid2 expression increases to the same level as that in mESC-S while the Eed expression remains at a low level (Fig. S4A, 4B). The rescue of Jarid2 expression is further confirmed by the qRT-PCR and WB analysis at both mRNA and protein levels (Fig. S4C,4D). The ChIP-seq analyses demonstrated that the global Ezh2 occupancy and histone H3K27me3 modification are partially restored along with the partial rescue of global Jarid2 occupancy in the mESCs cultured in the 2i medium (Fig. 4A-4D). Based on these results, we concluded that the reduced Jarid2 expression in primitive mESCs is the main molecular mechanism leading to the reduction of global PRC2 occupancy and histone H3K27me3 modification in primitive mESCs.

5. Global reduced PRC2 occupancy does not cause de-repression of early differentiation genes in primitive mESCs

To examine whether the reduced PRC2 occupancy leads to transcriptional de-repression of its regulated lineage differentiation genes in primitive mESCs, we extracted a total of 2567 unique PRC2-regulated genes based on their promoters bound by Ezh2 and examined their expression in mESCs cultured in serum-containing medium versus 2i medium. The ChIP-seq results confirmed that both Ezh2 occupancy and histone H3K27me3 modification around the transcription start sites (TSS) of these genes are decreased but partially restored after Jarid2 is ectopically expressed in the mESCs cultured in 2i medium (Fig. S5A-5C). Compared to mESC-S, mESC-2i have a total 193 upregulated and 339 downregulated genes, while mESC-2i with ectopic Jarid2 expression have total 200 upregulated and 315 downregulated genes (cutoff: 1.5-fold expression change and $p < 0.01$) (Fig. 5A, 5B). Among these genes, 255 genes are commonly downregulated in the mESCs cultured in 2i medium, which is regardless of the overall levels of Jarid2, PRC2 occupancy, and histone H3K27me3 modification at their promoters, suggesting the reduced expression of these genes only depends on the 2i culture condition but not the levels of PRC2 occupancy and H3K27me3 modification (Fig. 5C, 5D). Importantly, the gene ontology (GO) analysis showed that these common downregulated genes have enriched GO terms involved in cell differentiation, which include multiple early lineage differentiation genes such as Gata6, Dab1, Dab2, and Sox11 (Fig. 5E-5G, Table S2). In contrast, the common upregulated genes in the mESCs cultured in 2i medium have enriched GO terms involved in transcriptional regulation, cytoskeleton organization, and cell migration (Fig. S5D-5F, Table S3). Based on these results, we concluded that the lineage differentiation genes are not de-repressed in the mESCs cultured in 2i medium even though their promoter-bound PRC2 and histone H3K27me3 modification are decreased.

Discussion

In mammalian cells PRC1 and PRC2 are recruited unmethylated CGIs and mediate histone H2AK119ub1 and histone H3 lysine 27 modification respectively. The overall effect of PRCs-mediated histone modifications is to increase transcriptional threshold, which is critical for maintaining mESCs in an undifferentiated state by preventing stochastic transcriptional activation of lineage differentiation genes.

Although the molecular mechanisms for recruiting PRCs to unmethylated CGIs in mammalian cells are not fully elucidated, previous studies have revealed that both Jarid2 and Mtf2 are required for the recruitment of PRC2(*8-13*), while Kdm2b recruits the PRC1.1 variant to unmethylated CGIs due to its CxxC-ZF domain binding to unmethylated CG-rich DNA

sequences(*14-16*). Recently, Kdm2b was also reported to recruit PRC2 to the DNA demethylated pericentric heterochromatin though the interaction of Jarid2 with Kdm2b/PRC1.1-meidated histone H2AK119ub1(*17*).

Compared to the mESCs cultured in serum-containing medium, the primitive mESCs in 2i medium have a reduced basal expression level of early differentiation genes(*19, 20*). Unexpectedly, the PRC2-mediated histone H3K27me3, which functions as a major epigenetic mechanism mediating the lineage-specific gene silencing in mESCs, was found to have a global reduction in primitive mESCs(*24, 25*). Although the exact mechanisms causing the reduced global PRC2 occupancy in primitive mESCs are unclear, based on the finding that primitive mESCs have a global DNA demethylation due to the loss of DNA methylation maintenance, one postulated mechanism is that Kdm2b binds to the new DNA demethylated regions and attracts PRC2 away from its canonical CGI binding sites(*26*).

For the first time, this study provided multiple lines of evidence to demonstrate that the genome-wide decreased PRC2 occupancy and histone H3K27me3 modification in primitive mESCs are caused by the reduced Jarid2-mediated PRC2 recruitment but not the Kdm2b-mediated PRC2 re-localization. First, the RNA-seq, qRT-PCR, and WB analyses found both Jarid2 and Eed have significant deceased expression in primitive mESCs, while Kdm2b and other Polycomb components have similar expression between mESC-S and mESC-2i (Fig. 1, S1). Jarid2 is a known factor to recruit PRC2 to CGIs in mammalian cells, while Eed plays a critical role in determining the overall H3K27me3 level by binding and propagating H3K27me3 modification in cells(*30*). Therefore, the decreased expression of Jarid2 and Eed provides an important molecular basis for the global reduced PRC2 occupancy and the H3K27me3 level in primitive mESCs. Second, the FGF/MAPK signaling pathway positively regulates the expression of Jarid2 and Eed since the reactivation of this signaling pathway in primitive mESCs upregulates the expression of both Jarid2 and Eed at the mRNA and protein levels (Fig. 2, S2). Therefore, the blocking of the FGF/MAPK signaling pathway in primitive mESCs decreases Jarid2 and Eed expression, which subsequently leads to overall reduction of PRC2 occupancy and histone H3K27me3 modification. Third, the ChIP-seq analyses showed the reduced global PRC2 occupancy and histone H3K27me3 modification at CGIs are corelated with global reduced Jarid2 occupancy. In contrast, both mESC-S and mESC-2i have the same Kdm2b occupancy at CGIs and a similar Ring1b occupancy at the center of CGIs (Fig. 3, S3). Since Kdm2b has the same expression level in mESC-S and mESC-2i (Fig. S1), these results indicated that Kdm2b is less likely to have

genome-wide re-localization in primitive mESCs. In addition, the histone H3K4me3 modification at CGIs, what is mainly mediated by Mll2 that binds to CGIs through a similar CxxC-ZF domain as Kdm2b, is increased at CGIs in primitive mESCs (Fig. S3)(*31*), further arguing against that the CxxC-ZF domain-containing proteins like Kdm2b are relocated from CGIs to the new DNA demethylated regions. Finally, ectopic expression of Jarid2 in primitive mESCs could partially rescue the global PRC2 occupancy and the histone H3K27me3 modification at CGIs (Fig. 4, S4) further supporting that the reduced Jarid2-mediated PRC2 recruitment is the main causing factor leading to the genome-wide reduction of PRC2 occupancy in primitive mESCs.

The reduced PRC2 binding at gene promoters normally leads to de-repression of its regulated lineage-specific genes in mESCs cultured in serum-containing medium, in which mESCs express low-level lineage-specific transcription factors. However, the RNA-seq analyses in this study showed that the PRC2-regulated early lineage-specific genes remain silenced or downregulated even though their promoter-bound PRC2 and histone H3K27me3 are decreased in primitive mESCs (Fig. 5, S5). These results suggest that only transcription factors, but not the PRC2-mediated histone modification, play a dominant role in determining transcriptional activation. In the absence of transcription factors in primitive mESCs, the reduced PRC2-mediated epigenetic modification at gene promoters is not sufficient to turn on the transcription of lineage-specific genes.

Of note, recent studies reported that the developing oocytes and preimplantation mouse embryos lose the typical histone H3K27me3 modification at gene promoters(*32, 33*). It will be interesting to examine whether the mechanisms revealed by this study play any roles in determining the overall PRC2 occupancy and H3K27me3 modification in oocytes and preimplantation embryos in vivo, as well as its functional role in the epigenomic reprogramming during germline and preimplantation embryonic development.

Supplementary Materials

Materials and Methods
Fig. S1. The expression of Jarid2 and Eed expression is significantly reduced in primitive mESCs.
Fig. S2. FGF/MAPK signaling positively regulates the expression of Jarid2 and Eed.
Fig. S3. The genome-wide PRC2 occupancy is largely reduced in primitive mESCs.
Fig. S4. Ectopic expression of Jarid2 partially restores the global PRC2 occupancy and histone H3K27me3 modification in primitive mESCs.

Fig. S5. Global reduced PRC2 occupancy does not cause de-repression of early differentiation genes in primitive mESCs.
Table S1. Result of KEGG pathway analysis on the genes upregulated in response to the reactivation of FGF/MAPK signaling.
Table S2. Result of gene ontology analysis on the common PRC2-regulated genes that are downregulated in both mESC-2i and mESC-2i with ectopically expressed Jarid2.
Table S3. Sequences of all primers used in this study.

References

1. L. A. Boyer *et al.*, Polycomb complexes repress developmental regulators in murine embryonic stem cells. *Nature* **441**, 349-353 (2006).
2. L. Aloia, B. Di Stefano, L. Di Croce, Polycomb complexes in stem cells and embryonic development. *Development* **140**, 2525-2534 (2013).
3. T. I. Lee *et al.*, Control of developmental regulator's by polycomb in human embryonic stem cells. *Cell* **125**, 301-313 (2006).
4. R. Cao *et al.*, Role of histone H3 lysine 27 methylation in Polycomb-group silencing. *Science* **298**, 1039-1043 (2002).
5. H. Wang *et al.*, Role of histone H2A ubiquitination in Polycomb silencing. *Nature* **431**, 873-878 (2004).
6. L. Di Croce, K. Helin, Transcriptional regulation by Polycomb group proteins. *Nat Struct Mol Biol* **20**, 1147-1155 (2013).
7. E. M. Riising *et al.*, Gene silencing triggers polycomb repressive complex 2 recruitment to CpG islands genome wide. *Mol Cell* **55**, 347-360 (2014).
8. D. Landeira *et al.*, Jarid2 is a PRC2 component in embryonic stem cells required for multi-lineage differentiation and recruitment of PRC1 and RNA Polymerase II to developmental regulators. *Nat Cell Biol* **12**, 618-624 (2010).
9. D. Pasini *et al.*, JARID2 regulates binding of the Polycomb repressive complex 2 to target genes in ES cells. *Nature* **464**, 306-310 (2010).
10. X. Shen *et al.*, Jumonji modulates polycomb activity and self-renewal versus differentiation of stem cells. *Cell* **139**, 1303-1314 (2009).
11. M. Casanova *et al.*, Polycomblike 2 facilitates the recruitment of PRC2 Polycomb group complexes to the inactive X chromosome and to target loci in embryonic stem cells. *Development* **138**, 1471-1482 (2011).
12. H. Li *et al.*, Polycomb-like proteins link the PRC2 complex to CpG islands. *Nature* **549**, 287-291 (2017).
13. O. Oksuz *et al.*, Capturing the Onset of PRC2-Mediated Repressive Domain Formation. *Mol Cell* **70**, 1149-1162 e1145 (2018).
14. X. Wu, J. V. Johansen, K. Helin, Fbxl10/Kdm2b recruits polycomb repressive complex 1 to CpG islands and regulates H2A ubiquitylation. *Mol Cell* **49**, 1134-1146 (2013).
15. J. He *et al.*, Kdm2b maintains murine embryonic stem cell status by recruiting PRC1 complex to CpG islands of developmental genes. *Nat Cell Biol* **15**, 373-384 (2013).
16. A. M. Farcas *et al.*, KDM2B links the Polycomb Repressive Complex 1 (PRC1) to recognition of CpG islands. *Elife* **1**, e00205 (2012).
17. S. Cooper *et al.*, Targeting Polycomb to Pericentric Heterochromatin in Embryonic Stem Cells Reveals a Role for H2AK119u1 in PRC2 Recruitment. *Cell Rep* **7**, 1456-1470 (2014).
18. A. G. Smith, Embryo-derived stem cells: of mice and men. *Annu Rev Cell Dev Biol* **17**, 435-462 (2001).
19. Q. L. Ying *et al.*, The ground state of embryonic stem cell self-renewal. *Nature* **453**, 519-523 (2008).

20. J. Silva *et al.*, Promotion of reprogramming to ground state pluripotency by signal inhibition. *PLoS Biol* **6**, e253 (2008).
21. S. Takahashi, S. Kobayashi, I. Hiratani, Epigenetic differences between naive and primed pluripotent stem cells. *Cell Mol Life Sci* **75**, 1191-1203 (2018).
22. H. G. Leitch *et al.*, Naive pluripotency is associated with global DNA hypomethylation. *Nat Struct Mol Biol* **20**, 311-316 (2013).
23. F. von Meyenn *et al.*, Impairment of DNA Methylation Maintenance Is the Main Cause of Global Demethylation in Naive Embryonic Stem Cells. *Mol Cell* **62**, 983 (2016).
24. H. Marks *et al.*, The transcriptional and epigenomic foundations of ground state pluripotency. *Cell* **149**, 590-604 (2012).
25. G. Guo *et al.*, Serum-Based Culture Conditions Provoke Gene Expression Variability in Mouse Embryonic Stem Cells as Revealed by Single-Cell Analysis. *Cell Rep* **14**, 956-965 (2016).
26. M. Walter, A. Teissandier, R. Perez-Palacios, D. Bourc'his, An epigenetic switch ensures transposon repression upon dynamic loss of DNA methylation in embryonic stem cells. *Elife* **5**, (2016).
27. G. Guo *et al.*, Klf4 reverts developmentally programmed restriction of ground state pluripotency. *Development* **136**, 1063-1069 (2009).
28. M. Yamaji *et al.*, PRDM14 ensures naive pluripotency through dual regulation of signaling and epigenetic pathways in mouse embryonic stem cells. *Cell Stem Cell* **12**, 368-382 (2013).
29. S. Munoz Descalzo, P. Rue, J. Garcia-Ojalvo, A. Martinez Arias, Correlations between the levels of Oct4 and Nanog as a signature for naive pluripotency in mouse embryonic stem cells. *Stem Cells* **30**, 2683-2691 (2012).
30. R. Margueron *et al.*, Role of the polycomb protein EED in the propagation of repressive histone marks. *Nature* **461**, 762-767 (2009).
31. S. Denissov *et al.*, Mll2 is required for H3K4 trimethylation on bivalent promoters in embryonic stem cells, whereas Mll1 is redundant. *Development* **141**, 526-537 (2014).
32. H. Zheng *et al.*, Resetting Epigenetic Memory by Reprogramming of Histone Modifications in Mammals. *Mol Cell* **63**, 1066-1079 (2016).
33. Q. Xu, W. Xie, Epigenome in Early Mammalian Development: Inheritance, Reprogramming and Establishment. *Trends Cell Biol* **28**, 237-253 (2018).
34. B. Langmead, S. L. Salzberg, Fast gapped-read alignment with Bowtie 2. *Nat Methods* **9**, 357-359 (2012).
35. Y. Zhang *et al.*, Model-based analysis of ChIP-Seq (MACS). *Genome Biol* **9**, R137 (2008).
36. F. Ramirez, F. Dundar, S. Diehl, B. A. Gruning, T. Manke, deepTools: a flexible platform for exploring deep-sequencing data. *Nucleic Acids Res* **42**, W187-191 (2014).
37. J. T. Robinson *et al.*, Integrative genomics viewer. *Nat Biotechnol* **29**, 24-26 (2011).
38. D. Kim *et al.*, TopHat2: accurate alignment of transcriptomes in the presence of insertions, deletions and gene fusions. *Genome Biol* **14**, R36 (2013).

Acknowledgments: Funding: This work was supported by the National Institute Health NIH grant R01GM127431. **Author contributions:** J.H. conceived the project. M.B.A., Y.G. and J.H. designed and performed the experiments. J.H. and G.I.M. performed the sequencing data analysis. J.H. interpreted the data and wrote the manuscript. **Competing interests:** The authors declare no competing interests.

Figures and Figure Legend

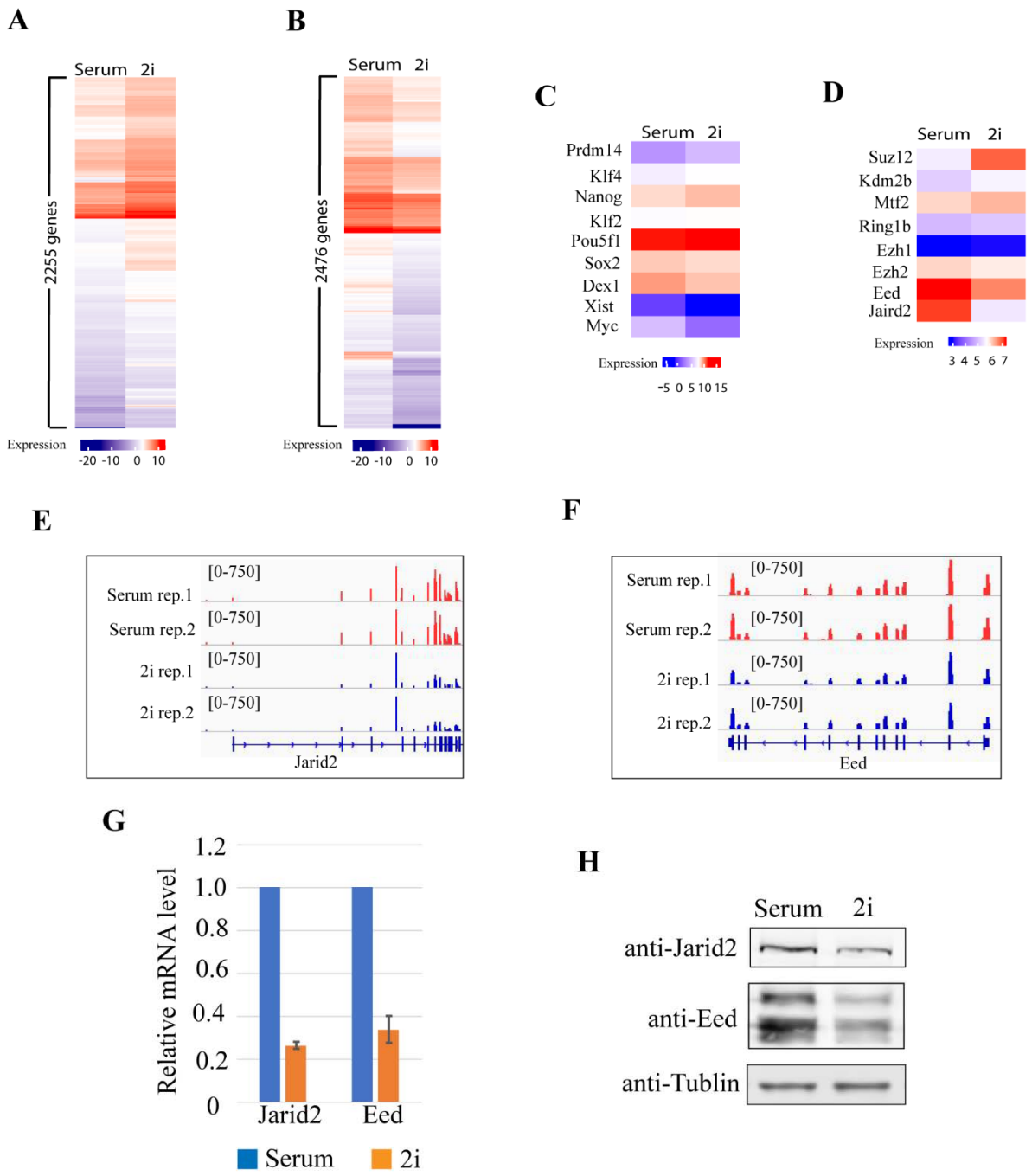

Figure 1. The expression of Jarid2 and Eed expression is significantly reduced in primitive mESCs. (**A**) Heatmap showing 2255 genes upregulated in mESC-2i. (**B**) Heatmap showing 2476 genes downregulated in mESC-2i. (**C**) Heatmap showing the expression of genes known to be up- and down-regulated in mESC-2i. (**D**) Heatmap showing the expression of Polycomb genes in mESC-S and mESC-2i. The expression of Jarid2 and Eed is significantly reduced in mESC-2i. (**E**) The IGV genome browser view of Jarid2 expression in mESC-S and mESC-2i. (**F**) The IGV genome browser view of Eed expression in mESC-S and mESC-2i. (**G**) qRT-PCR analysis showing Jarid2 and Eed have a reduced mRNA level in mESC-2i. The results were normalized against levels of Gapdh and the expression level in mESC-S was arbitrarily set to 1. (**H**) Western blot analysis showing Jarid2 and Eed have a reduced protein level in mESC-2i.

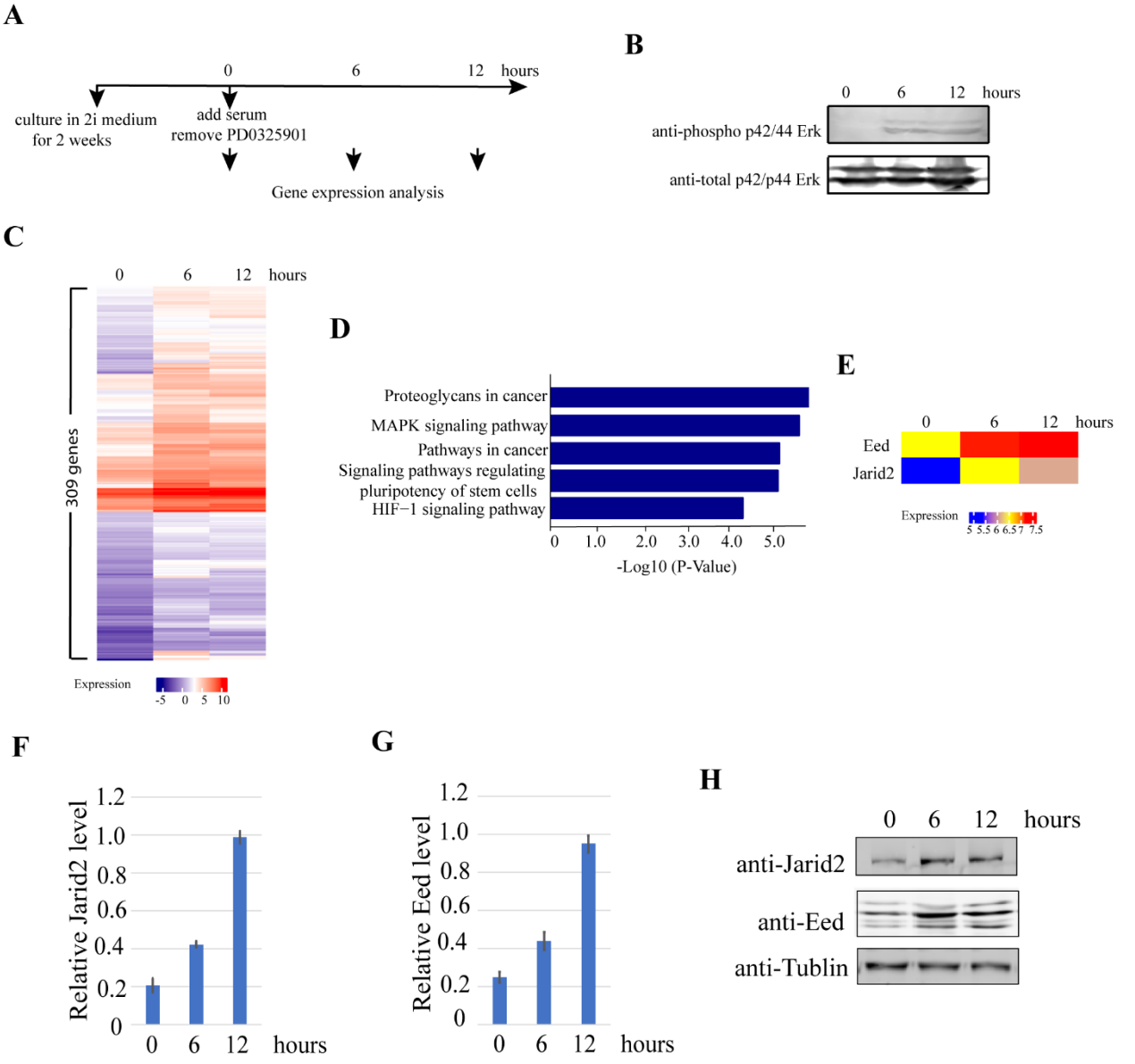

Figure 2. FGF/MAPK signaling positively regulates the expression of Jarid2 and Eed. (**A**) Schematic showing the experimental design for the analysis of gene expression in response to the reactivation of FGF/MAPK signaling pathway. (**B**) Western blot analysis showing phosphorylated p42/44 MAPK is increased 6 hours after the reactivation of FGF/MAPK signaling. (**C**) Heatmap showing 309 genes are upregulated in response to the reactivation of FGF/MAPK signaling. (**D**) KEGG signal pathway analysis showing the five top signaling pathways that are activated in response to the reactivation of FGF/MAPK signaling. (**E**) Heatmap showing both Jarid2 and Eed are upregulated in response the reactivation of FGF/MAPK signaling. (**F**) qRT-PCR analysis showing Jarid2 expression is upregulated at the mRNA level in response to the reactivation of FGF/MAPK pathway. The results were normalized against levels of Gapdh and the expression level in mESC-S was arbitrarily set to 1. (**G**) qRT-PCR analysis showing Eed expression is upregulated at the mRNA level in response to the reactivation of FGF/MAPK pathway. The results were normalized against levels of Gapdh and the expression level in mESC-S was arbitrarily set to 1. (**H**) Western blot analysis showing both Jarid2 and Eed are upregulated at the protein level in response to the reactivation of FGF/MAPK pathway.

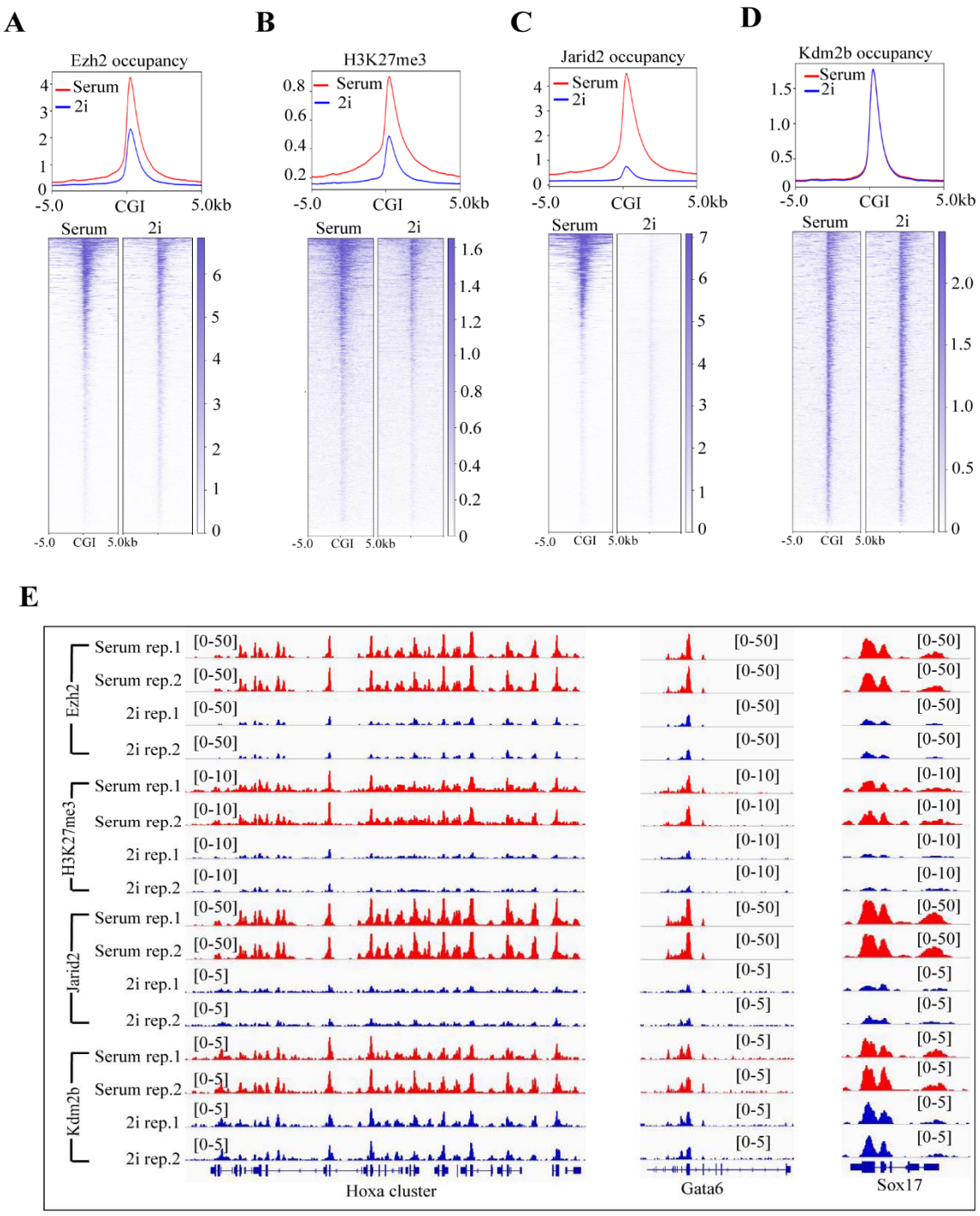

Figure 3. The genome-wide PRC2 occupancy is largely reduced in primitive mESCs. (**A**) The plot (upper) and heatmap (bottom) showing the Ezh2 occupancy within 10kb-window flanking CGIs in mESC-S and mESC-2i. (**B**) The plot (upper) and heatmap (bottom) showing the histone H3K27me3 modification within 10kb-window flanking CGIs in mESC-S and mESC-2i. (**C**) The plot (upper) and heatmap (bottom) showing the Jarid2 occupancy within 10kb-window flanking CGIs in mESC-S and mESC-2i. (**D**) The plot (upper) and heatmap (bottom) showing the Kdm2b occupancy within 10kb-window flanking CGIs in mESC-S and mESC-2i. (**E**) The IGV genome browser view of Ezh2, Jarid2, Kdm2b occupancy and histone H3K27me3 modification at the representative Hoxa gene locus (left panel), Gata6 (middle panel), and Sox17 (right panel). The red color represents the level in mESC-S (serum) and the blue color represents the level in mESC-2i (2i).

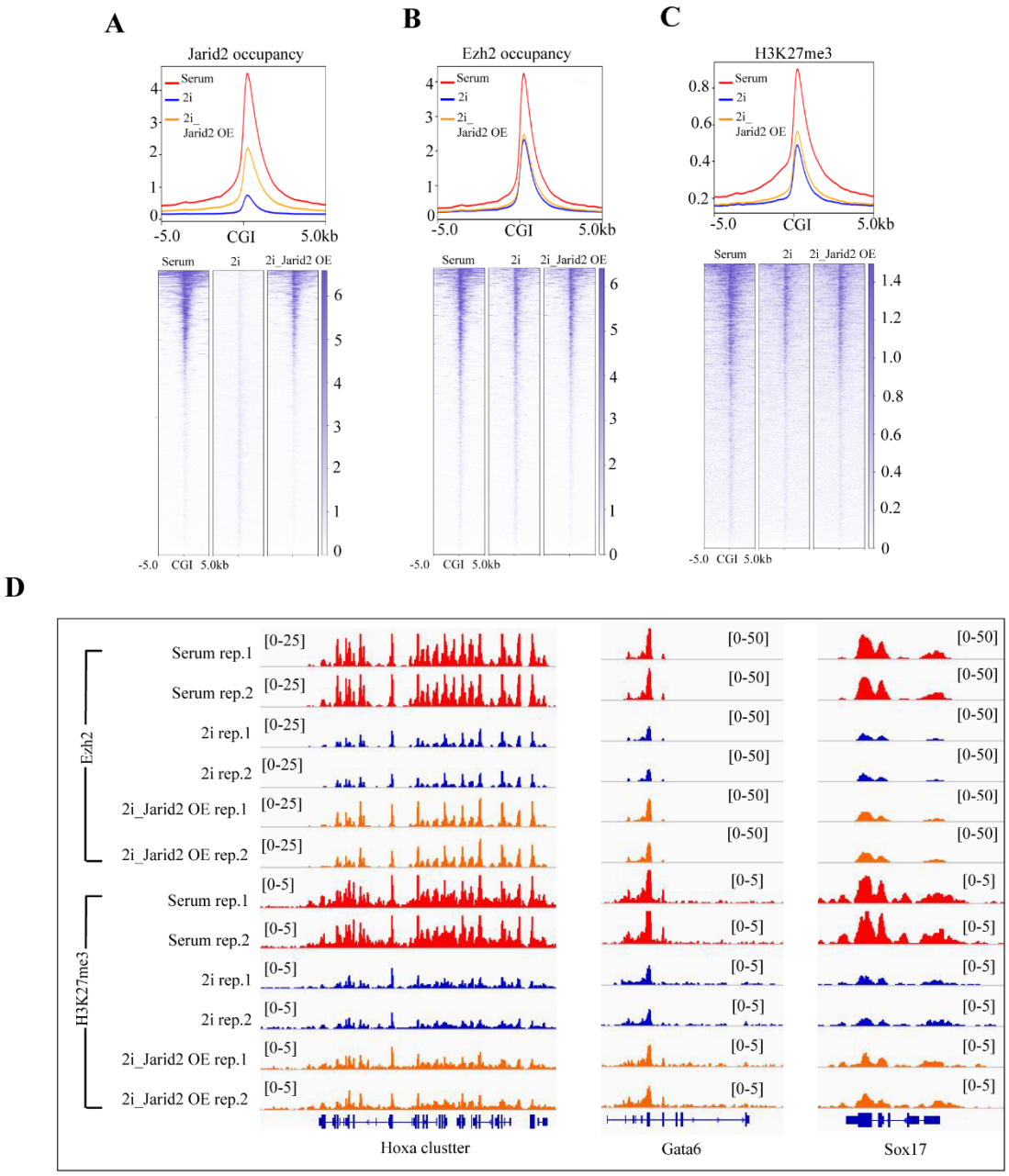

Figure 4. Ectopic expression of Jarid2 partially restores the global PRC2 occupancy and histone H3K27me3 modification in primitive mESCs. (**A**) The plot (upper) and heatmap (bottom) showing the Jarid2 occupancy within 10kb-window flanking CGIs in mESC-S (serum), mESC-2i (2i), and mESC-2i with ectopically expressed Jarid2 (2i_Jarid OE). (**B**) The plot (upper) and heatmap (bottom) showing the Ezh2 occupancy within 10kb-window flanking CGIs in mESC-S (serum), mESC-2i (2i), and mESC-2i with ectopically expressed Jarid2 (2i_Jarid2_OE). (**C**) The plot (upper) and heatmap (bottom) showing the histone H3k27me3 within 10kb-window flanking CGIs in mESC-S (serum), mESC-2i (2i), and mESC-2i with ectopically expressed Jarid2 (2i_Jarid2 OE). The red line represents the level in mESC-S (serum), the blue line represents the level in mESC-2i (2i), and the orange line represents the level in mESC-2i with ectopically expressed Jarid2 (2i_Jarid OE). (**D**) The IGV genome browser view of Ezh2 and histone H3K27me3 modification at the representative Hoxa gene locus (left panel), Gata6 (middle panel), and Sox17 (right panel). The red color represents the level in mESC-S (serum), the blue color represents the level in mESC-2i (2i), and the orange color represents the level in level in mESC-2i with ectopically expressed Jarid2 (2i_Jarid OE).

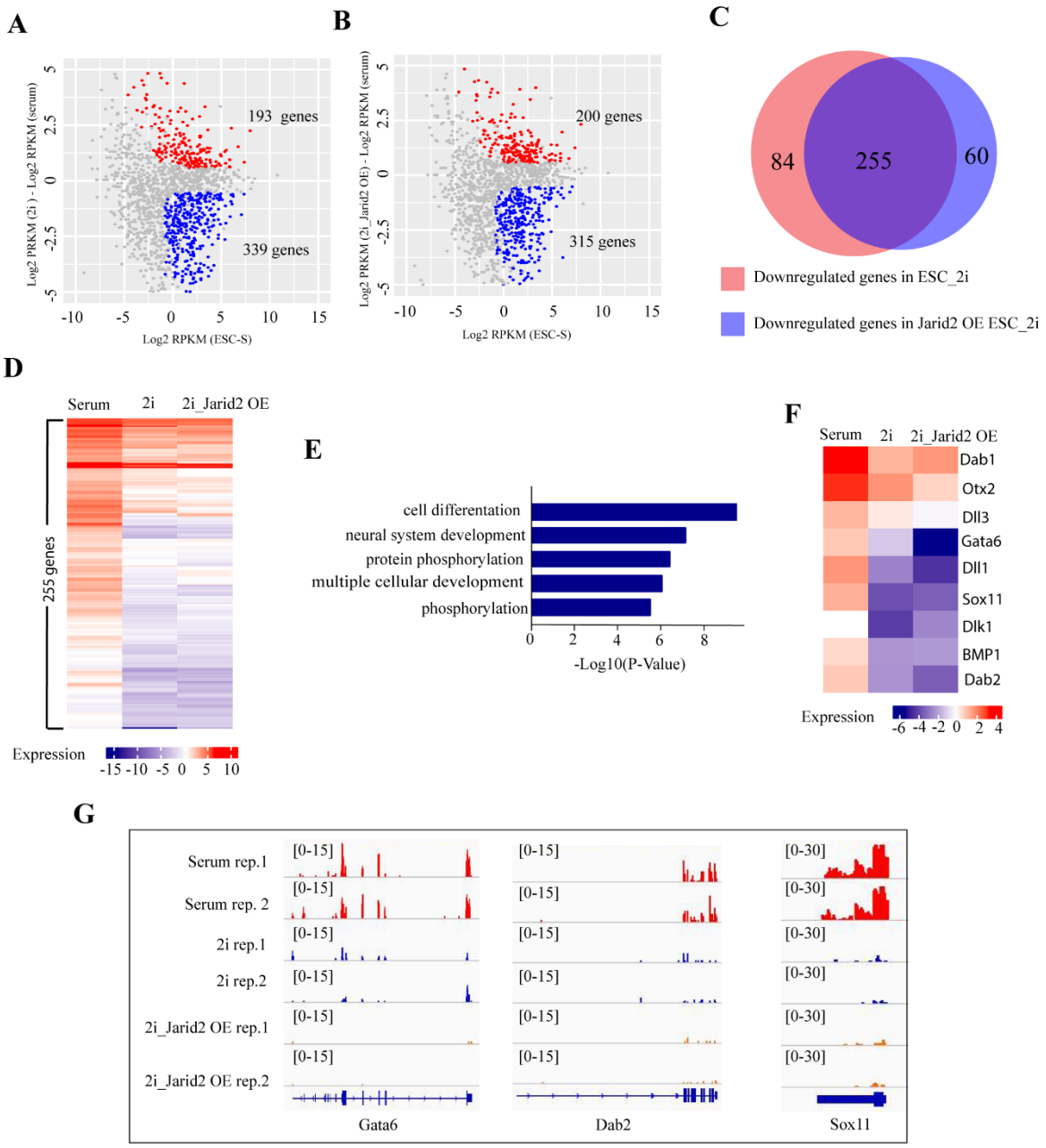

Figure 5. Global reduced PRC2 occupancy does not cause de-repression of early differentiation genes in primitive mESCs. (**A**) RNA-seq results showing significant 193 up- and 339 down-regulated PRC2-bound genes in mESC-2i compared to that in mESC-S. (**B**) RNA-seq results showing significant 200 up- and 315 down-regulated PRC2-bound genes in the mESC-2i with ectopically expressed Jarid2 compared to that in mESC-S. (**C**) A Venn diagram showing the common downregulated genes in the mESC-2i and in the mESC-2i with ectopically expressed Jarid2. The common downregulated genes are indicated by the overlapped area in the diagram. (**D**) Heatmap showing the 255 common downregulated genes in the mESC-2i (2i) and the mESC-2i with ectopically expressed Jarid2 (2i_Jarid OE) compared to mESC-S (serum). (**E**) Gene ontology analysis showing the enriched GO terms of 255 common downregulated genes in the mESC-2i and in the mESC-2i with ectopically expressed Jarid2. (**F**) A subset of early lineage differentiation genes downregulated in the mESC-2i and the mESC-2i with ectopically expressed Jarid2. (**G**) The IGV genome browser view of normalized RNA-seq reads (FPKM) of lineage differentiation genes Gata6 (left panel), Dab2 (middle panel), and Sox11 (right panel) in mESC-S, mESC-2i, and mESC-2i with ectopically expressed Jarid2.

Supplementary Materials

Materials and Methods

Mouse embryonic stem cell culture

The wild-type E14 mESC line and wild-type E14 mESCs with 3xFlag knock-in to the endogenous Kdm2b gene(*15*) were maintained on the 0.1% gelatin coated plates in "2i" medium that contained 50% Neurobasal medium (Life Technologies) and 50% DMEM/F12 medium (Life Technologies) supplemented with 1x N2-supplement (Gibco), 1x B27 supplement (Gibco), 7.5% bovine serum albumin (Gibco), 1x GlutaMAX (Life Technologies), 1x beta-mercaptoethanol (Life Technologies), 1mM PD03259010, 3mM CHIR99021, 1000 units/ml leukemia inhibitory factor (ESGRO, EMD Millipore), and 100U/ml penicillin/streptomycin (Life Technologies). The serum-containing mESC culture condition included DMEM medium (Life Technologies) supplemented with 100U/ml penicillin/streptomycin (Life Technologies), 15% fetal bovine serum (Sigma), 1x nonessential amino acid, 1x sodium pyruvate (Life Technologies), 1x GlutaMAX (Life Technologies), 1x beta-mercaptoethanol (Life Technologies) and 1000 units/ml leukemia inhibitory factor (ESGRO, EMD Millipore).

Western Blot analysis

Total proteins were extracted by RIPA buffer and separated by electrophoresis by 8-10% PAGE gel. The protein was transferred to the nitrocellulose membrane and blotted with primary antibodies. The antibodies used for Western Blot and IP-Western Blot analyses included: rabbit anti-Flag (1:2000, Cell Signaling Technology); rabbit anti-Ezh2 (1:1000 Cell Signaling Technology); rabbit anti-Ring1B (1:1000, Cell Signaling Technology); rabbit anti-Suz12 (1:1000 Cell Signaling Technology); rabbit anti-Jarid2 ((1:1000, Santa Cruz Biotechnology); rabbit anti-p42/44 MAPK (1:1000 Cell Signaling Technology); rabbit anti-phospho-p42/44 MAPK ((1:1000 Cell Signaling Technology) and rabbit anti-Mtf2 (1:1000, Proteintech), and IRDye 680 donkey anti-rabbit second antibody (1: 10000, Li-Cor). The images were developed by Odyssey Li-Cor Imager (Li-Cor).

RT-qPCR assays

RNA was extracted and purified from cells using QI shredder (Qiagen) and RNeasy (Qiagen) spin columns. Total RNA (1 µg) was subjected to reverse transcription using Iscript reverse transcription supermix (Bio-Rad). cDNA levels were assayed by real-time PCR using iTaq

universal SYBR green supermix (Bio-Rad) and detected by CFX386 Touch Real-Time PCR detection system (Bio-Rad). Primer sequences for qPCR are listed in Supplementary Table 3.

ChIP-Seq sample preparation

For Ezh2, Jarid2, Ring1b, Kdm2b, H3K27me3 and H3K4me3 ChIP, Kdm2b 3xFlag knock-in wild-type E14 cells(*15*) were fixed with 2mM Ethylene glycol bis[succinimidylsuccinate] (Thermo Scientific) for 1 hour, followed by 10 min in 1% formaldehyde and 5 min 0.125 M glycine to sequence the reaction. Cells were lysed in 1% SDS, 10 mM EDTA, 50 mMTris-HCl (pH 8.0) and the DNA was fragmented to approximately 200-400 bp by sonification (Branson Sonifier 450). Immunoprecipitation was performed with 3 µg rabbit polyclonal anti-Flag (Sigma), rabbit anti-Ezh2 antibody (1:100, Cell Signaling Technology), rabbit anti-Jarid2 antibody (1:100, Cell Signaling Technology), rabbit anti-Ring1b antibody (1:100, Cell Signaling Technology), 2ug rabbit anti-H3K27me3 antibody (Diagenode), 2ug rabbit anti-H3K4me4 antibody (Diagenode) overnight at 4°C. Antibody bound DNA-proteins were isolated by protein G plus/protein A agarose beads (EMD Millipore), washed, eluted and reverse cross-linked DNA was extracted by phenol/chloroform and precipitated.

ChIP DNA preparation for HiSeq4000 sequencing

ChIP DNA library was constructed for HiSeq4000 (Illumina) sequencing using NEBNext UltraII DNA library Prep Kit for Illumina (New England BioLabs, Inc) according to the manufacturer's instructions. Adapter-ligated DNA was amplified by PCR for 12-14 cycles and followed by size selection using agarose gel electrophoresis. The DNA was purified using QIAquick gel extraction kit (Qiagen) and quantified both with an Agilent Bioanalyzer and Invitrogen Qubit. The DNA was diluted to a working concentration of 20nM prior to sequencing. Sequencing on an Illumina HiSeq4000 instrument was carried out by the Genomics Core Facility at Michigan State University.

ChIP-Seq data analysis

For the ChIP-Seq data analysis, all sequencing reads were mapped to NCBI build 37 (mm9) of the mouse genome using Bowtie2(*34*). Mapped reads were analyzed using the MACS program and bound-regions (peaks) were determined using sequencing reads from input DNA as negative controls(*35*). When multiple reads mapped to the same genomic position, a maximum of two reads were retained. The statistical cutoff used for peak calling was P-value$< 10^{-8}$ and >5-fold enrichment over the control. The mapped sequencing reads were normalized as Counts Per

Million Reads (CPM). The normalized reads were binned into 50-bp windows along the genome using the bamCoverage of deepTools program and visualized in the IGV genome browser(*36, 37*). The datasets of CpG islands and Refseq genes of mm9 were retrieved from the UCSC table bowser. The heatmap and plot of ChIP-seq reads in the 10kb-windows flanking CGIs or Refseq genes were generated using plotHeatmap and plotProile in the deepTools program. The subset of Refseq genes regulated by PRC2 were determined by the 2kb promoter regions upstream of transcriptional start site overlapped with Ezh2-bound regions.

RNA-seq sample preparation for HiSeq4000 sequencing

RNA was extracted and purified from cells using QI shredder (Qiagen) and RNeasy (Qiagen) spin columns. Total RNA (1 µg) was used to generate RNA-seq library using NEBNext Ultra Directional RNA library Prep Kit for Illumina (New England BioLabs, Inc) according to the manufacturer's instructions. Adapter-ligated cDNA was amplified by PCR and followed by size selection using agarose gel electrophoresis. The DNA was purified using Qiaquick gel extraction kit (Qiagen) and quantified both with an Agilent Bioanalyzer and Invitrogen Qubit. The libraries were diluted to a working concentration of 10nM prior to sequencing. Sequencing on an Illumina HiSeq4000 instrument was carried out by the Genomics Core Facility at Michigan State University.

RNA-Seq data analysis

RNA-Seq data analysis was performed essentially as described previously. All sequencing reads were mapped mm9 of the mouse genome using Tophat2(*38*). The mapped reads were normalized to reads as Reads Per Kilobase of transcript per Million mapped reads (RPKM). The differential gene expression was calculated by Cuffdiff program and the statistic cutoff for identification of differential gene expression is $p < 0.01$ and 1.5-fold RPKM change between samples. The normalized mapped reads (RPKM) of each RNA-seq experiments were binned into 50bp windows along the genome using the bamCoverage of deepTools program and visualized in the IGV genome browser. The heatmap and plot of gene expression were generated using plotHeatmap and plotProile in the deepTools program. The differential expressed gene lists were input into the DAVID Functional Annotation Bioinformatics Microarray Analysis for KEGG pathway and gene ontology enrichment analyses (https://david.ncifcrf.gov/).

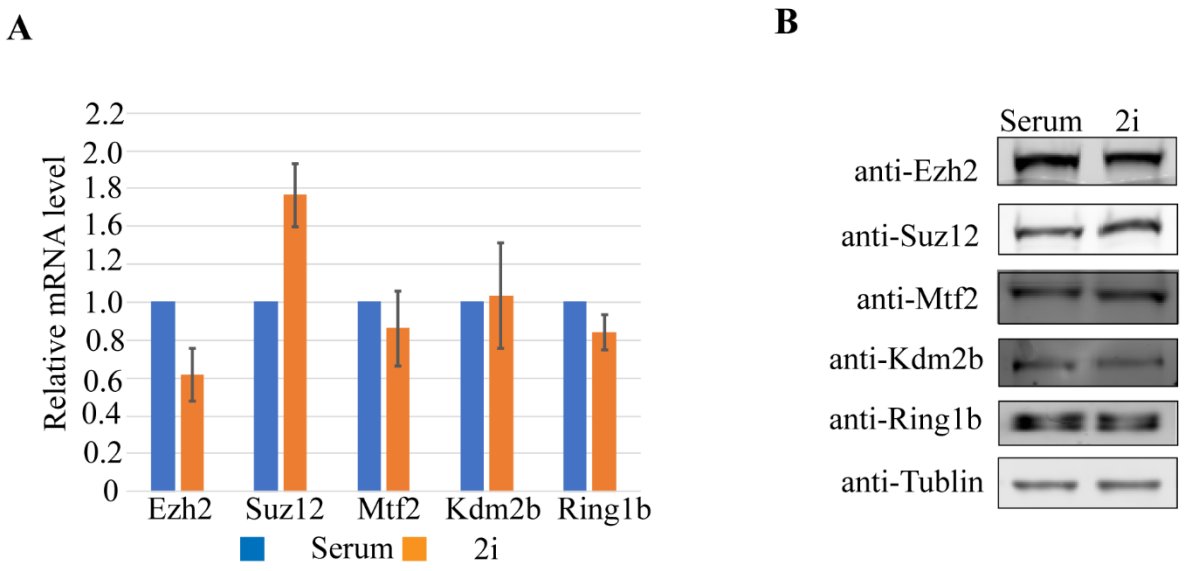

Figure S1. The expression of Jarid2 and Eed expression is significantly reduced in primitive mESCs. (**A**) qRT-PCR analysis showing the expression level of Ezh2, Suz12, Mtf2, Kdm2b, and Ring1b in mESC-S (serum) and mESC-2i (2i). The results were normalized against levels of Gapdh and the mRNA level in mESC-S was arbitrarily set to 1. (**B**) Western blot analysis showing the protein level of Ezh2, Suz12, Mtf2, Kdm2b, and Ring1b in mESC-S (serum) and mESC-2i (2i).

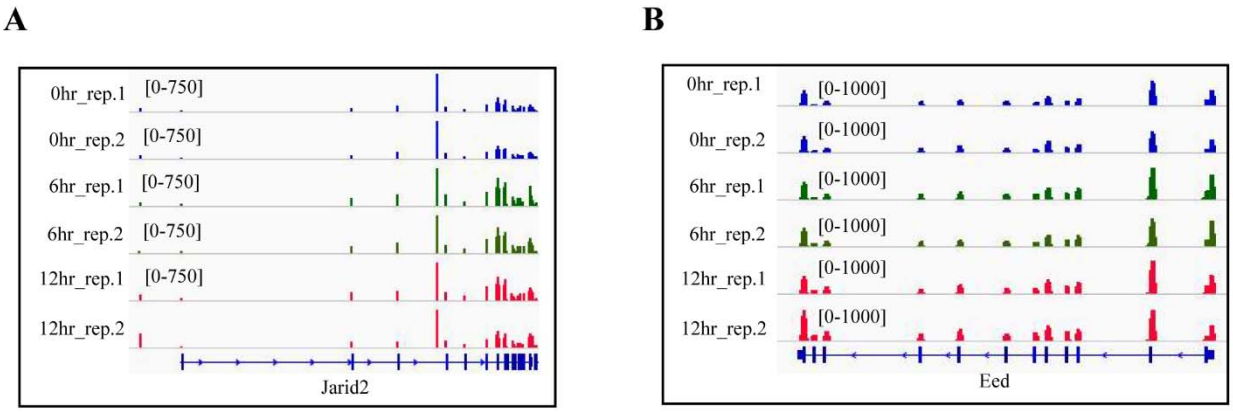

Figure S2. FGF/MAPK signaling positively regulates the expression of Jarid2 and Eed. (**A**) The IGV genome browser view of Jarid2 expression before, 6 hours and 12 hours after the reactivation of FGF/MAPK signaling pathway. (**B**) The IGV genome browser view of Eed expression before, 6 hours and 12 hours after the reactivation of FGF/MAPK signaling pathway.

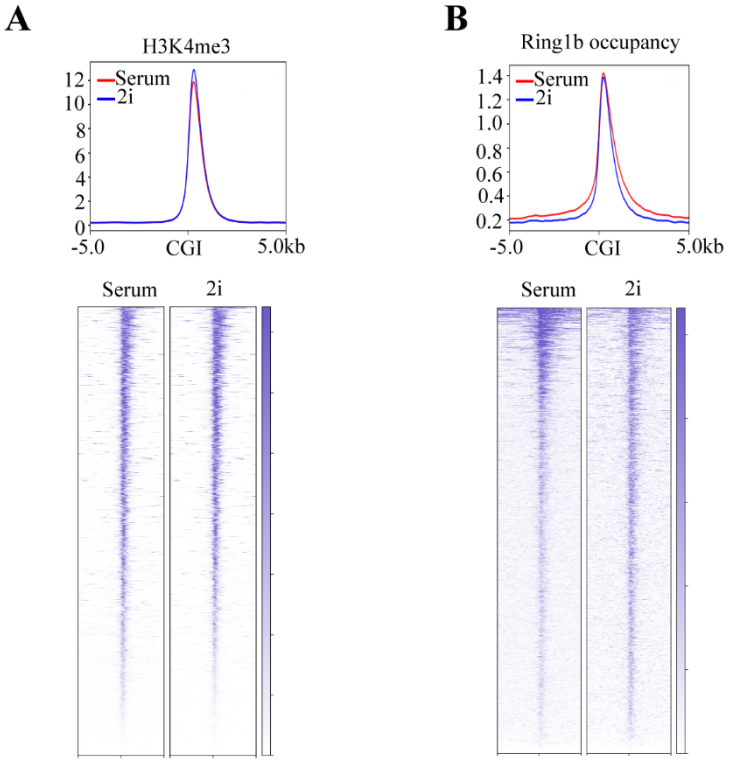

Figure S3. The genome-wide PRC2 occupancy is largely reduced in primitive mESCs. (**A**) The plot (upper) and heatmap (bottom) showing the histone H3K4me3 modification within 10kb-window flanking CGIs in mESC-S and mESC-2i. (**B**) The plot (upper) and heatmap (bottom) showing the Ring1b occupancy within 10kb-window flanking CGIs in mESC-S and mESC-2i.

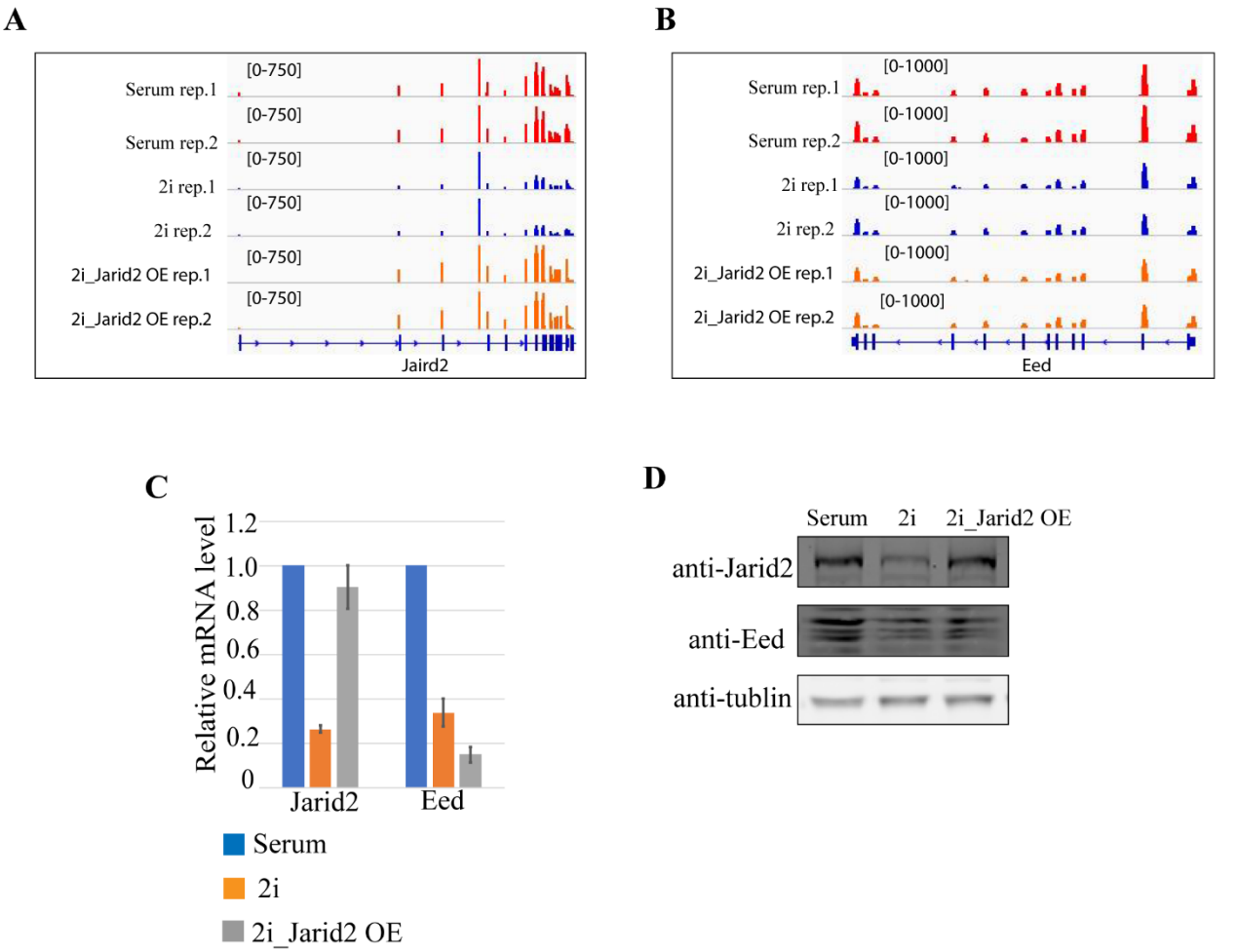

Figure S4. Ectopic expression of Jarid2 partially restores the global PRC2 occupancy and histone H3K27me3 modification in primitive mESCs. (**A**) The IGV genome browser view of Jarid2 expression in mESC-S (serum), mESC-2i (2i), and mESC-2i with ectopically expressed Jarid2 (2i_Jarid2_OE). (**B**) The IGV genome browser view of Eed expression in mESC-S (serum), mESC-2i (2i), and mESC-2i with ectopically expressed Jarid2 (2i_Jarid2_OE). (**C**) qRT-PCR analysis showing Jarid2 and Eed mRNA level in mESC-S (serum), mESC-2i (2i), and mESC-2i with ectopically expressed Jarid2 (2i_Jarid2_OE). The results were normalized against levels of Gapdh and the expression level in mESC-S was arbitrarily set to 1. (**D**) Western blot analysis showing both Jarid2 and Eed protein level in mESC-S (serum), mESC-2i (2i), and the mESC-2i with ectopically expressed Jarid2 (2i_Jarid2_OE).

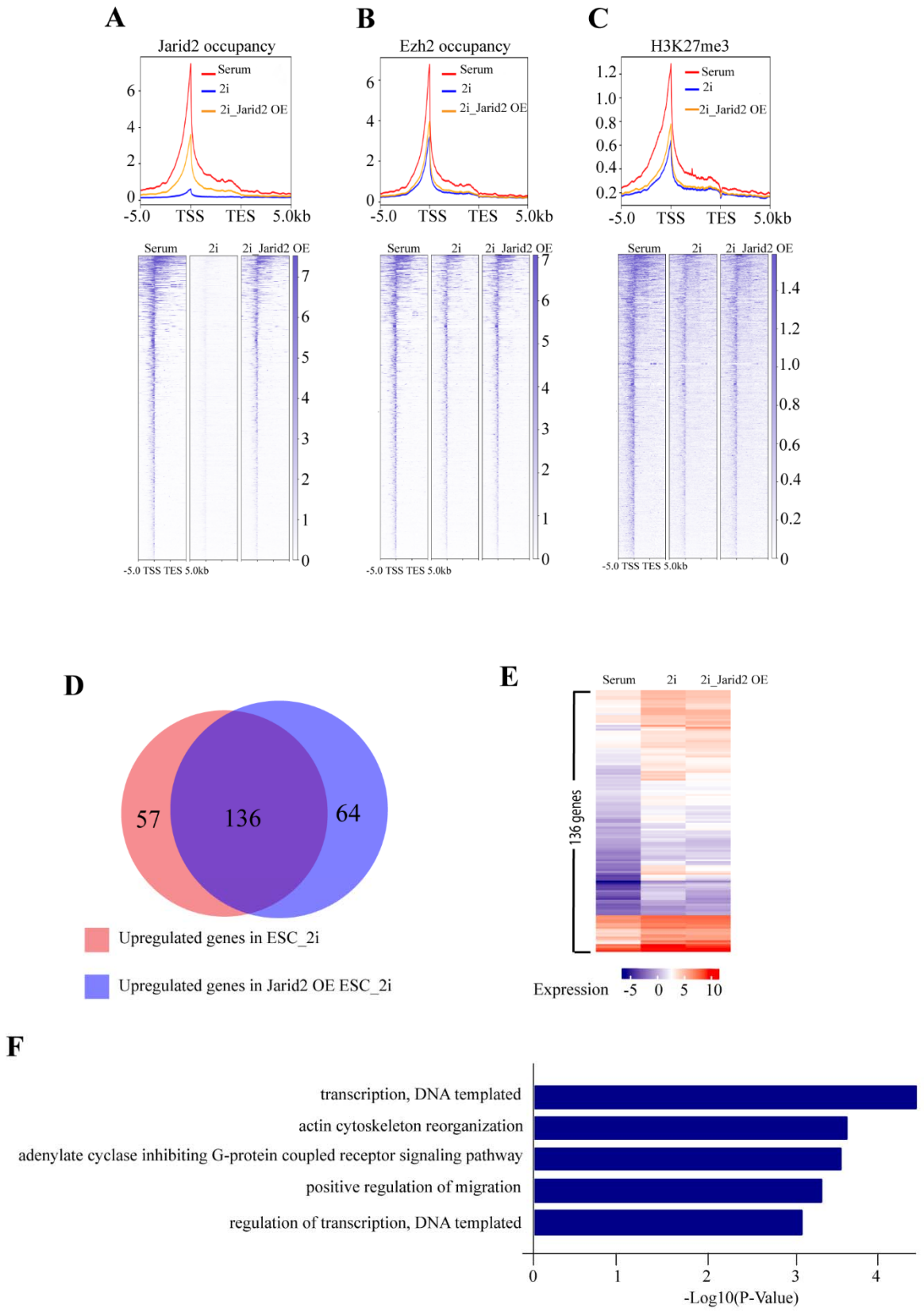

Figure S5. Global reduced PRC2 occupancy does not cause de-repression of early differentiation genes in primitive mESCs. (**A**) The plot (upper) and heatmap (bottom) showing the Jarid2 occupancy within 10kb-window flanking the PRC2-regulated genes in mESC-S (serum), mESC-2i (2i), and mESC-2i with ectopically expressed Jarid2 (2i_Jarid OE). (**B**) The plot (upper) and heatmap (bottom) showing the Ezh2 occupancy within 10kb-window flanking

the PRC2-regulated genes in mESC-S (serum), mESC-2i (2i), and mESC-2i with ectopically expressed Jarid2 (2i_Jarid2_OE). (**C**) The plot (upper) and heatmap (bottom) showing the histone H3k27me3 modification within 10kb-window flanking the PRC2-regulated genes in mESC-S, mESC-2i, and mESC-2i with ectopically expressed Jarid2. The red line represents the level in mESC-S (serum), the blue line represents the level in mESC-2i (2i), and the orange line represents the level in mESC-2i with ectopically expressed Jarid2 (2i_Jarid OE). TSS: Transcriptional Start Sites; TES: Transcription End Sites. (**D**) A Venn diagram showing the common upregulated PRC2-bound genes in the mESC-2i and in the mESC-2i with ectopically expressed Jarid2. The common upregulated genes are indicated by the overlapped area in the diagram. (**E**) Heatmap showing 136 common upregulated PRC2-bound genes in the mESC-2i and the the mESC-2i (2i) with ectopically expressed Jarid2 ((2i_Jarid OE) compared to mESC-S (serum). (**F**) Gene ontology analysis showing the enriched GO terms of 136 common upregulated genes in the mESC-2i and the mESC-2i with ectopically expressed Jarid2.